ELSEVIER

Polymer 40 (1999) 1979–1984

polymer

Phase behaviors of solid polymer electrolytes: applicability of an extended Debye–Hückel theory

Jung Yong Kim, Young Chan Bae*

Department of Industrial Chemistry and Molecular Thermodynamics Laboratory, Hanyang University, Seoul 133-791, South Korea

Received 16 February 1998; revised 11 May 1998; accepted 25 May 1998

Abstract

Poly(ethylene oxide) (PEO) with three different salts, $ZnCl_2$, $ZnBr_2$ and ZnI_2 has been characterized at various temperatures and compositions by optical microscopy and differential scanning calorimetry. A molecular thermodynamic model based on both an extended Flory–Huggins theory and a Debye–Hückel theory modified by Guggenheim is developed to interpret the liquidus curves in the resulting phase diagram. The proposed model considers not only short-range specific interactions between the salt ions and the polymer or solvating base groups (oxygen in PEO) of the polymer leading to loose complex formation but also long-range electrostatic forces between salt ions. Quantitative description according to the proposed model is in good agreement with experimentally observed transition temperature of a given system including an eutectic point.

Keywords: Melting point depression; Extended Flory–Huggins theory; Extended Debye–Hückel theory; Eutectic point

1. Introduction

Polymer electrolyte, i.e. the ionic conductors resulting from the complexation of poral polymers with low-lattice-energy salts, has been the subject of many studies. Most recent research and development activities have been focused on the identification of solid polymer electrolytes (SPE) with sufficiently high ionic conductivity to allow the operation of solid-state Li batteries at ambient temperature with rates similar to those of their liquid electrolyte-based counterpart. SPE has been proposed for a wide variety of extremely demanding applications, such as electric vehicle, start–light–ignition, and portable electronic and personal communication [1–3].

Initial studies of SPE have focused on PEO-based Li(I) electrolytes, however recent investigations have shown that PEO dissolves a wide range of salts of monovalent, divalent and trivalent cations [4]. For example, Blumberg et al. [5] reported that PEO forms complexes with MCl_2 (M = Cd, Hg). Wissburn and Hannon [6] presented the view that inorganic nitrates such as $M(NO_3)_2$ (M = Ca, Cu, Zn, Cd) are quite soluble in the polymers, namely, cellulose acetate, poly(vinyl acetate), poly(vinly alcohol), poly(methyl methacrylate) and poly(methyl acrylate). James et al. [7] studied poly(propylene oxide) and found that it forms single-phase amorphous complex with MX_2 (M = Fe, Co, Cu, Zn; X = Cl, Br, I). Fontanella et al. [8] characterized PEO complexes with $Ba(SCN)_2$ and $Ca(SCN)_2$. More recently, Farrington et al. [4,9,10] extensively studied PEO complexes with MX_2 (M = Mg, Ca, Cu, Zn, Ni, Pb; X = Cl, Br, I) and applied molecular simulations to PEO/LiBr, PEO/$ZnBr_2$.

Phase diagrams appear to be an appropriate descriptive approach for a better understanding of the conductivity, stability and mechanical properties, and as such have been the objective of several studies to determine the domain of existence as a function of salt type, composition and temperature. For example, Shriver et al. [11] constructed the phase diagram for the PEO/NH_4SCN system. Lee and Crist [12] reported the phase behavior of PEO/NaSCN mixtures which form eutectic reactions. Fauteux et al. [13–15] studied extensively phase behaviors of binary SPE systems such as PEO/LiX (X = $CF_3SO_3^-$, ClO_4^-, AsF_6^-, $N(CF_3SO_2)_2^-$, $C(CF_3SO_3)_3^-$) and PEO/NaI. Gorecki et al. [16] described the phase diagram of PEO/Li [$(CF_3SO_2)_2N$] from the physics point of view. Kim et al. [17] established the phase diagrams of PEO/$MnBr_2$, PEO/MnI_2 and compared their experimental results with a thermodynamic model which considers only salt ion–polymer interactions.

In this study, we presented phase diagrams of PEO/ZnX_2 (X = Cl, Br, I) as model systems. We combined an extended Flory–Huggins theory [17–19] and an extended Debye–

* Corresponding author.

0032-3861/99/$ - see front matter
PII: S0032-3861(98)00415-7

Hückel theory developed by Guggenhiem [20,21]. An advantage of the extended Debye–Hückel theory is its simplicity in calculating the liquidus curves in the phase diagram of the binary polymer/salt systems, where salt cation, salt anion and polymer repeating unit are assumed to occupy one cell in a lattice, respectively. PEO is able to dissolve large concentrations of ionic salts because of strong salt ion–polymer interactions that overcome the lattice energies of the salts. The extended Debye–Hückel theory [20,21] assumes that salts dissociate completely and the consequential increase in the ion–ion interactions should be corrected in an optimization factor which is chosen to be universal to all polymer/salt systems. The extended Flory–Huggins theory [17–19] does not take into account the difference between salt cation and salt anion.

2. Model development

Three theoretical aspects are taken into account: the lattice notation of a Debye–Hückel type function proposed by Guggenheim [20,21], the modification of an extended Flory–Huggins equation [17–19] and Flory's melting point depression concept [22].

The total molar Gibbs energy of mixing $\Delta G_{\mathrm{mix}}^{\mathrm{Total}}$ is assumed to consist of an extended Debye–Hückel (DH) theory and an extended Flory–Huggins (FH) theory:

$$\frac{\Delta G_{\mathrm{mix}}^{\mathrm{Total}}}{\mathrm{R}T}=\frac{\Delta G_{\mathrm{mix}}^{\mathrm{DH}}}{\mathrm{R}T}+\frac{\Delta G_{\mathrm{mix}}^{\mathrm{FH}}}{\mathrm{R}T} \tag{1}$$

where R is the gas constant and T is the absolute temperature.

2.1. A lattice notation of an extended Debye–Hückel theory

For a binary polymer/salt system at solute molality m (mole/kg polymer), Guggenheim's expression for the molar Gibbs energy of mixing $\Delta G_{\mathrm{mix}}^{\mathrm{DH}}$ could be rewritten in the framework of lattice theory as follows [20,21]:

$$\frac{\Delta G_{\mathrm{mix}}^{\mathrm{DH}}}{\mathrm{R}T}=\frac{\phi_1}{r_1 v m}\left[-\frac{4}{3}AI^{3/2}\tau\left(I^{1/2}\right)\right] \tag{2}$$

$$\tau(x)=\frac{3}{x^3}\left[\ln(1+x)-x+\frac{x^2}{2}\right] \tag{3}$$

where ϕ_1 is the segment fraction of the salt ion, r_1 (= 1) is the number of segments per salt ion, v (= $v_M + v_X$; v_M and v_X are the number of M and X ions, respectively, per salt) is the number of ions per salt, and I is the ionic strength. A is the usual Debye–Hückel coefficient. In this study we fix $A = 0.068$ (assumed to be independent of temperature) as an optimization factor for polymer/salt systems. This small value implies that ion–ion interactions in a polymer/salt system are relatively small (for example, calculated percentage at molality of salt $\approx$ 0.1 mol/kg in PEO/$LiCF_3SO_3$ system: ions = 2%; pairs = 71%; triples = 27%) [1]. For a binary polymer/salt system containing 1 kg of polymer and vm moles of salt ion, ϕ_1 and I are defined by

$$\phi_1=\frac{r_1 v m}{r_1 v m+r_2 1000/M}=\frac{r_1 N_1}{r_1 N_1+r_2 N_2},\ \phi_2=1-\phi_1 \tag{4}$$

$$I=\frac{1}{2}mv|z_M z_X|=\frac{1}{2}\left[\frac{r_2\phi_1 1000/M}{r_1\phi_2}\right]\cdot|z_M z_X| \tag{5}$$

where M is the molecular weight of polymer in g/mol (i.e. M = 900 000 g/mol). N_1, N_2, z_M, z_X and r_2 are the number of moles of salt ion and polymer, the valences of M and X ions and the number of segments per polymer, respectively. The chemical potentials are given by

$$\frac{\Delta\mu_1^{\mathrm{DH}}}{\mathrm{R}T}=\frac{1}{\mathrm{R}T}\left(\frac{\partial(r_1N_1+r_2N_2)\Delta G_{\mathrm{mix}}^{\mathrm{DH}}}{\partial N_1}\right)$$
$$=-\frac{v}{1000}\left(\frac{A|z_M z_X|I^{1/2}}{1+I^{1/2}}\right) \tag{6}$$

$$\frac{\Delta\mu_2^{\mathrm{DH}}}{\mathrm{R}T}=\frac{1}{\mathrm{R}T}\left(\frac{\partial(r_1N_1+r_2N_2)\Delta G_{\mathrm{mix}}^{\mathrm{DH}}}{\partial N_2}\right)$$
$$=\frac{M}{1000}\left(\frac{2}{3}AI^{3/2}\sigma(I^{1/2})\right) \tag{7}$$

$$\sigma(x)=\frac{3}{x^3}\left[1+x-\left(\frac{1}{1+x}\right)-2\ln(1+x)\right] \tag{8}$$

2.2. The extended Flory–Huggins theory

For a binary polymer/salt system, the Flory–Huggins expression for the molar Gibbs energy of mixing $\Delta G_{\mathrm{mix}}^{\mathrm{FH}}$ at a temperature T is given by [22]

$$\frac{\Delta G_{\mathrm{mix}}^{\mathrm{FH}}}{\mathrm{R}T}=\frac{\phi_1}{r_1}\ln\phi_1+\frac{\phi_2}{r_2}\ln\phi_2+\chi_{\mathrm{FH}}\phi_1\phi_2 \tag{9}$$

where χ_{FH} is the Flory–Huggins interaction parameter. Recently, Qian et al. [19,23] suggested a semiempirical form for χ. They replaced χ_{FH} by $g(T,\phi_2)$, a function of temperature and concentration. The Gibbs free energy of mixing and chemical potentials in terms of the new interaction parameter χ from the relation $\chi = g - \phi_1 g'$, are given by

$$\frac{\Delta G_{\mathrm{mix}}^{\mathrm{FH}}}{\mathrm{R}T}=\frac{1-\phi_2}{r_1}\ln(1-\phi_2)+\frac{\phi_2}{r_2}\ln\phi_2+\phi_2\int_{\phi_2}^{1}\chi(T,\phi)\mathrm{d}\phi \tag{10}$$

$$\frac{\Delta\mu_1^{\mathrm{FH}}}{\mathrm{R}T}=\ln(1-\phi_2)+\phi_2\left(1-\frac{r_1}{r_2}\right)+\chi(T,\phi_2)r_1\phi_2^2 \tag{11}$$

$$\frac{\Delta\mu_2^{\mathrm{FH}}}{\mathrm{R}T}=\ln\phi_2+(1-\phi_2)\left(1-\frac{r_2}{r_1}\right)-r_2\phi_1\phi_2\chi(T,\phi_2)$$
$$+r_2\int_{\phi_2}^{1}\chi(T,\phi)\mathrm{d}\phi \tag{12}$$

Qian et al. proposed that χ is given by the product of a temperature-dependent term, $D(T)$, and a concentration-dependent term, $B(\phi)$ [24]:

$$\chi(T,\phi) = D(T)B(\phi_2) \tag{13}$$

In this study, we use simple functions of temperature and composition reported elsewhere [17]:

$$D(T) = d_0 + \frac{d_1}{T} \tag{14}$$

$$B(\phi_2) = 1 + b\phi_2 \tag{15}$$

where d_0, d_1 and b are adjustable model parameters.

2.3. The melting point depression theory

In a semicrystalline system, the condition of equilibrium between crystalline polymer and the polymer unit in the solution may be described as follows [22]:

$$\mu_u^c - \mu_u^0 = \mu_u - \mu_u^0 \tag{16}$$

where μ_u^c, μ_u and μ_u^0 are chemical potentials of crystalline polymer segment unit, of liquid (amorphous) polymer segment unit and chemical potential in the standard state, respectively. Now the formal difference appearing on the left-hand side is expressed as follows:

$$\mu_u^c - \mu_u^0 = -\Delta H_u(1 - T/T_m^0) \tag{17}$$

where ΔH_u is the heat of fusion per segment unit, T and T_m^0 are the melting temperature of the species in a mixture and of the pure phases, respectively. The right-hand side of Eq. (16) can be restated by substituting Eqs. (7) and (12) into Eq. (16) as follows:

$$\begin{aligned}\mu_u - \mu_u^0 &= \left(\Delta\mu_2^{DH} + \Delta\mu_2^{FH}\right)\frac{V_u}{V_1}\frac{r_1}{r_2} \\ &= RT\frac{V_u}{V_1}\left[\frac{r_1}{r_2}\frac{M}{1000}\left(\frac{2}{3}AI^{2/3}\sigma\left(I^{1/2}\right)\right)\right. \\ &\quad + \frac{r_1}{r_2}\ln\phi_2 + (1-\phi_2)\left(\frac{r_1}{r_2} - 1\right) \\ &\quad - r_1\phi_1\phi_2\left(d_0 + \frac{d_1}{T_{m,2}}\right)(1 + b\phi_2) \\ &\quad \left. + r_1\left(d_0 + \frac{d_1}{T_{m,2}}\right)\left(1 + \frac{b}{2} - \phi_2 - \frac{b}{2}\phi_2^2\right)\right]\end{aligned} \tag{18}$$

where V_u and V_1 are the molar volumes of the polymer repeating unit and of salt ions, respectively. By substituting Eqs. (17) and (18) into Eq. (16) and replacing T by $T_{m,2}$, the equilibrium melting temperature of the mixture is given by

$$\begin{aligned}\frac{1}{T_{m,2}} - \frac{1}{T_{m,2}^0} &= -\frac{R}{\Delta H_u}\frac{V_u}{V_1}\left[\frac{r_1}{r_2}\frac{M}{1000}\left(\frac{2}{3}AI^{2/3}\sigma(I^{1/2})\right)\right. \\ &\quad + \frac{r_1}{r_2}\ln\phi_2 + (1-\phi_2)\left(\frac{r_1}{r_2} - 1\right) \\ &\quad - r_1\phi_1\phi_2\left(d_0 + \frac{d_1}{T_{m,2}}\right)(1 + b\phi_2) \\ &\quad \left. + r_1\left(d_0 + \frac{d_1}{T_{m,2}}\right)\left(1 + \frac{b}{2} - \phi_2 - \frac{b}{2}\phi_2^2\right)\right]\end{aligned} \tag{19}$$

The subscripts 1, 2 and u refer to the salt ion, the polymer and the polymer segment unit, respectively. Similarly, we obtain

$$\begin{aligned}\frac{1}{T_{m,1}} - \frac{1}{T_{m,1}^0} &= -\frac{R}{\Delta H_1}\left[-\frac{v}{1000}\left(\frac{A|z_M z_X|I^{1/2}}{1 + I^{1/2}}\right)\right. \\ &\quad + \ln(1-\phi_2) + \phi_2\left(1 - \frac{r_1}{r_2}\right) \\ &\quad \left. + \left(d_0 + \frac{d_1}{T_{m,1}}\right)(1 + b\phi_2)r_1\phi_2^2\right]\end{aligned} \tag{20}$$

From Eqs. (19) and (20), we can predict liquidus curves in the phase diagram of binary polymer/salt systems.

3. Experimental

3.1. Sample preparation

Poly(ethylene oxide) ($M_w = 900\,000$) was obtained from Aldrich Chemical Co. and was used without further purification. Zinc chloride (99.999%), zinc bromide (99.999%), zinc iodide (98%) and acetonitrile (99.9%) were also supplied by Aldrich Chemical Co. and were used as received. Ethyl alcohol (EtOH) (99.9%) was supplied by Hayman Ltd.

For PEO/$ZnCl_2$, PEO/$ZnBr_2$ and PEO/ZnI_2 systems, samples were cast in mixed solvents. PEO was dissolved easily in acetonitrile and the salt is dissolved in EtOH. To form films, known amounts of PEO were dissolved in acetonitrile

Table 1
List of melting point temperature, heat of fusion, molecular weight, density and molar volume for each sample

	T_m^0 (K)	ΔH (cal/mole)	M.W. (g/mole)	Density (g/cm^3)	V (cm^3/mole)
PEO	338.15	1980[a]	900 000	1.21	36.60
$ZnCl_2$	556.15	1436.74	136.28	2.91	46.83
$ZnBr_2$	667.15	2501.63	225.19	4.20	53.60
ZnI_2	719.15	3985.93	319.18	4.74	67.39

[a]1980 cal/unit

Table 2
List of adjustable model parameters for given systems

	$PEO/ZnCl_2$		$PEO/ZnBr_2$		PEO/ZnI_2	
	$A = 0.0678$	$A = 0$	$A = 0.0678$	$A = 0$	$A = 0.0678$	$A = 0$
d_0	-0.104×10^2	-0.153×10^2	-0.197×10^2	-0.845×10^1	0.767×10^0	-0.338×10^1
d_1	0.303×10^4	0.813×10^4	0.601×10^4	0.386×10^4	-0.137×10^4	0.502×10^3
b	-0.142×10^1	-0.812×10^0	-0.120×10^1	-0.825×10^0	-0.816×10^0	-0.755×10^0

and zinc halides were dissolved in minimum amounts of EtOH. Acetonitrile solution then was mixed with EtOH solution. The mixture of various O/Zn mole ratios was stirred for 48 h at room temperature, and then cast on precleaned microscope slides (25 mm × 75 mm × 1 mm). Films were air-dried for several hours and then transferred to a vacuum oven. They were de-solvated under vacuum at 25°C for 24 h and then at 90°C for another 24 h. They were not used until crystallization was completed.

3.2. Thermo-optical analysis

Melting point measurements of polymer electrolyte/salt systems were carried out using a thermo-optical analysis (TOA) technique. It consists of a heating-cooling stage, a photodiode (Mettler FP80) and a microprocessor (Mettler FP90). The scan rate was 2.0°C/min. An IBM PC was used for data acquisition.

3.3. Differential scanning calorimetry

A Perkin-Elmer DSC-7 was used to measure the heat of fusion and melting temperature of pure salts at a heating rate of 10°C/min. The heat of fusion of $ZnCl_2$ (T_m^0: 283°C), $ZnBr_2$ (T_m^0: 394°C) and ZnI_2 (T_m^0: 446°C) are 44.11, 46.48 and 52.25 J/g, respectively.

4. Results and discussion

Fig. 1 shows the phase behavior of the $PEO/ZnCl_2$ system. Open circles were measured using TOA. The solid lines were predicted by the proposed model with $A = 0.068$. The dotted lines were calculated in the case of $A = 0$. The polymer-rich liquidus curve was calculated from Eq. (19) and the salt-rich curve was calculated from Eq. (20). The density of PEO was taken as 1.21 g cm^{-3}. The density of $ZnCl_2$ was 2.91 g cm^{-3}. By substituting values of $R = 1.98$ cal K^{-1} mol^{-1}, $\Delta H_1 = 1436.74$ cal mol^{-1}, $A = 0.068$, $z_M = 2$, $z_X = 1$, $r_1 = 1$, $r_2 = 20454.5$ and $T^0_{m,1} = 556.15$ K into Eq. (20), the best fit to the salt-rich liquidus curve (solid line on the right-hand side of Fig. 1) was obtained. Adjustable model parameters were $d_0 = -10.4$, $d_1 = 3032.73$ and $b = -1.42$. Substituting the same adjustable model parameters (d_0, d_1 and b) with $\Delta H_u = 1980$ cal mole^{-1}, $V_u = 36.6$ cm^3 mole^{-1}, $V_1 = 46.83$ cm^3 mole^{-1} and $T^0_{m,2} = 338.15$ K into Eq. (19) gives the solid line on the left-hand side of Fig. 1. As shown in Fig. 1, the theoretical prediction (solid lines) not only gives excellent agreement with the experimental results but also identifies the eutectic point at the intersection of the two liquidus curves at a weight fraction of $ZnCl_2 \approx 0.14$. The dotted line (an extended Flory–Huggins theory only, i.e. $A = 0$) shows some deviation from the experimental data, which is due

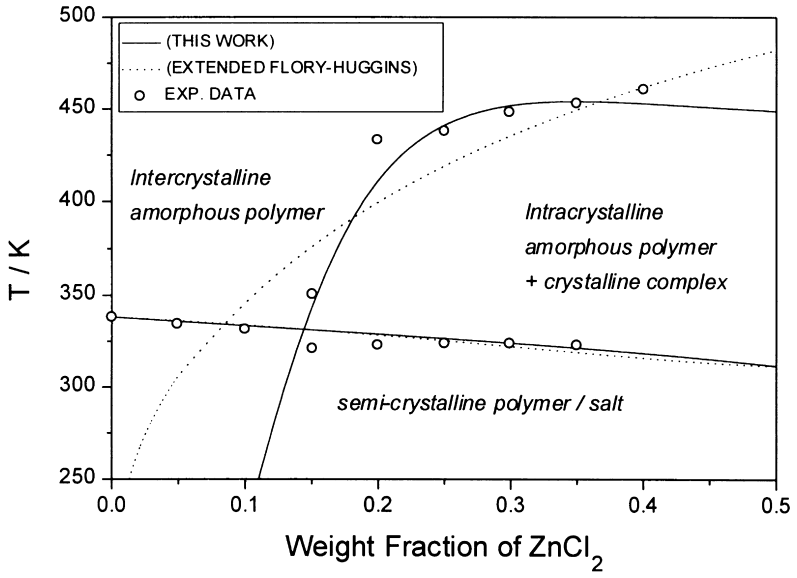

Fig. 1. Phase diagram of the $PEO/ZnCl_2$ system. The transition temperatures were obtained using a thermo-optical analysis technique (○). The solid lines are calculated from the proposed model. The dotted lines are calculated from the model based on an extended Flory–Huggins equation only.

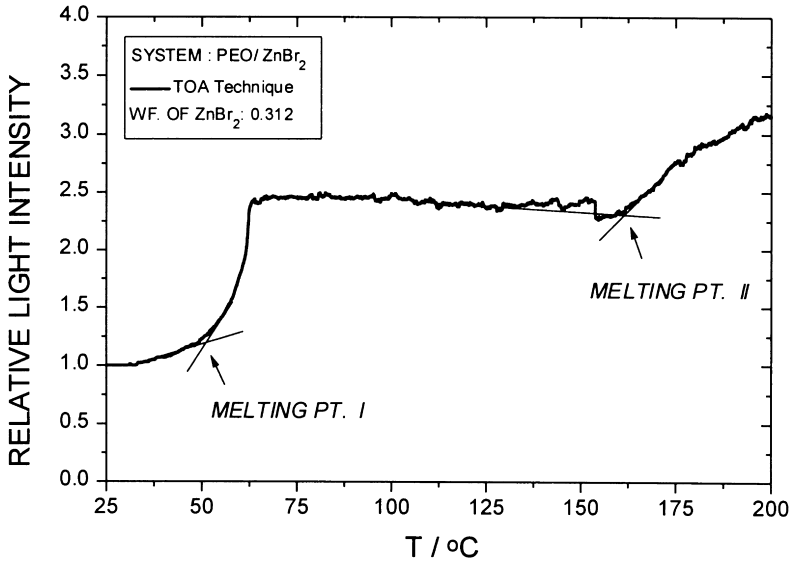

Fig. 2. A typical TOA result for determining the melting point temperature of a polymer/salt system. The model system is PEO/$ZnBr_2$ with a weight fraction of $ZnBr_2 \approx 0.312$. The scan rate was 2.0°C/min.

to the ignorance of long range electrostatic interactions between divalent zinc ions and monovalent bromide ions.

Fig. 2 shows how to determine two different melting points using the TOA technique for the PEO/$ZnBr_2$ system. The melting point I is approximately the same for all PEO–salt mixtures. The melting point II is attributed to the transition from intracrystalline amorphous polymer and crystalline complex to intercrystalline amorphous polymer.

Fig. 3 shows a phase behavior of the PEO/$ZnBr_2$ system. Open circles were measured by TOA. The solid lines were predicted by the proposed model (cf. Table 1, Table 2). The dotted lines were calculated by an extended Flory–Huggins model only (cf. Table 2). As shown in Fig. 3, the proposed model, being consistent with experimental data, identifies the eutectic point at a weight fraction of $ZnBr_2 \approx 0.15$. Melting points of this system in the salt-rich phase were more depressed than that of PEO/$ZnCl_2$, which could be explained by the degree of dissociation of salts based on the lattice enthalpy ($ZnCl_2 > ZnBr_2 > ZnI_2$).

Fig. 4 shows phase behaviors of the PEO/ZnI_2 system. Open circles were measured by TOA. The solid lines were predicted by the proposed model. The dotted lines were calculated by an extended Flory–Huggins model only. Based on the experimental results, we can expect an eutectic point to occur at a weight fraction of $ZnI_2 \approx 0.16$. However, theoretical prediction (eutectic point: $ZnI_2 \approx 0.11$) obtained by substituting the values from Tables 1 and 2 into Eqs. (19) and (20) shows a slight deviation from experimental results.

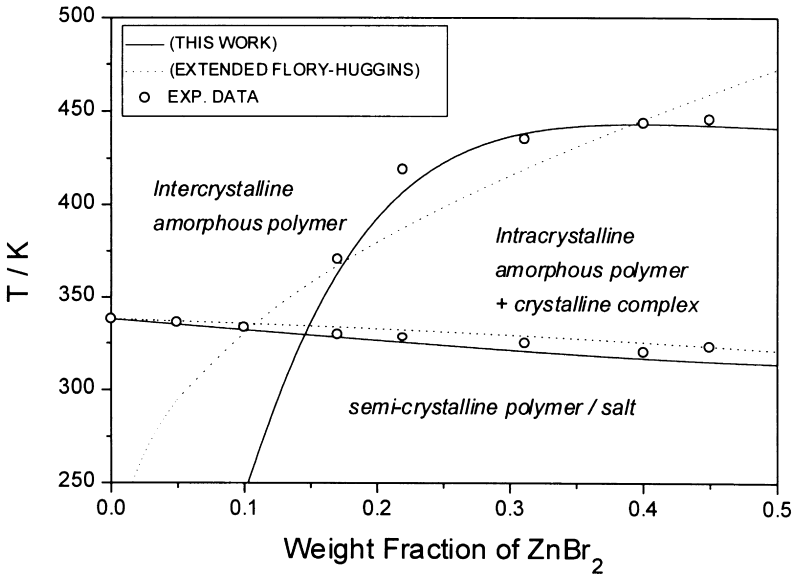

Fig. 3. Phase diagram of the PEO/$ZnBr_2$ system. The transition temperatures were obtained using a thermo-optical analysis technique (○). The solid lines are calculated from the proposed model. The dotted lines are calculated from the model based on an extended Flory–Huggins equation only.

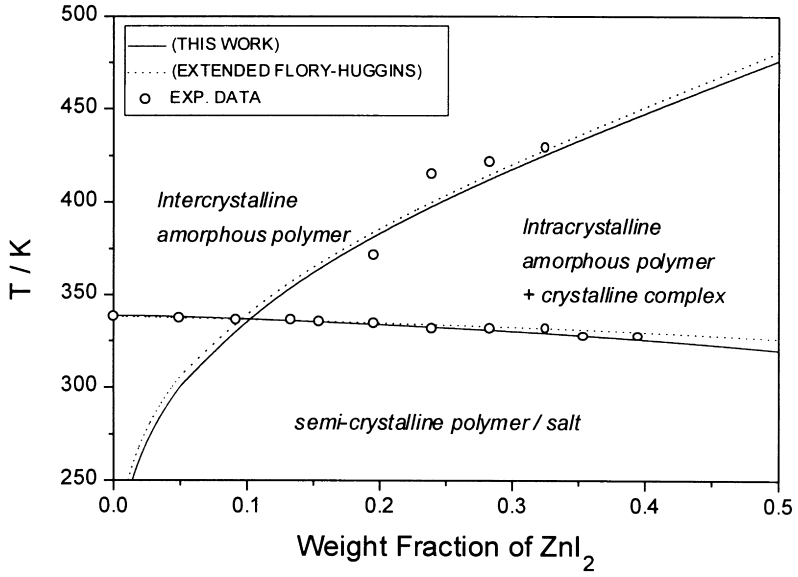

Fig. 4. Phase diagram of the PEO/ZnI_2 system. The transition temperatures were obtained using a thermo-optical analysis technique (○). The solid lines are calculated from the proposed model. The dotted lines are calculated from the model based on an extended Flory–Huggins equation only.

It might be due to the drastically depressed melting temperature of ZnI_2 ($T_m^0 = 719.15$ K), which phenomena is not easy to describe exactly by theoretical prediction.

5. Conclusions

The phase diagrams of SPE systems composed of PEO and zinc halides with relatively low lattice energy were constructed using thermal analysis such as TOA and DSC techniques. Eutectic points at the intersection of the two liquidus curves for PEO-based binary systems are at the weight fractions of $ZnCl_2 \approx 0.14$, $ZnBr_2 \approx 0.15$ and $ZnI_2 \approx 0.16$, respectively. The degree of melting point depression depends on intermolecular forces associated with salt type (lattice enthalpy; $ZnCl_2 > ZnBr_2 > ZnI_2$), PEO, compositions and thermal history. The proposed model considering both ion–polymer interactions (Flory–Huggins theory) and ion–ion interactions (Debye–Hückel theory modified by Guggenheim) describes very well the phase behaviors of polymer/salt systems.

Acknowledgements

This paper was supported by Research Fund (9606-060), the Korea Research Foundation, (December, 1996).

References

[1] MacCallum JR, Vincent CA. In: Polymer electrolyte reviews, Vols 1 and 2. Amsterdam: Elsevier, 1987/1989.
[2] Alamgir M, Abraham KM. In: Pistoia G, editor. Lithium batteries new materials, developments and perspectives, Vol. 5. Amsterdam: Elsevier, 1994:93.
[3] Fauteux D, Massucco A, Mclin M, Buren MV, Shi J. Electrochemica Acta 1995;40(13):2185.
[4] Yang H, Farrington GC. J Electrochem Soc 1992;139(6):1646.
[5] Blumberg AA, Pollack SS, Hoeve CAJ. J Polymer Sci (A) 1964;2:2499.
[6] Wissburn KF, Hennon MJ. J Polymer Sci Polym Phys Ed 1975;13:223.
[7] James DB, Wetton RE, Brown DS. Polymer 1979;20:187.
[8] Fontanella JJ, Wintersgill MC, Calame JP. J Polymer Sci Polym Phys Ed 1985;23:113.
[9] Huq R, Chiodelli G, Ferloni P, Magistris A, Farrington GC. J Electrochem Soc 1987;134(2):364.
[10] Xie L, Farrington GC. Solid State Ionics 1993;60:19.
[11] Stainer M, Hardy LC, Whitmore DH, Shriver DF. J Electrochem Soc 1984;131(4):784.
[12] Lee YL, Crist B. J Appl Phys 1986;60(8):2683.
[13] Robitaille CD, Fauteux D. J Electrochem Soc 1986;133(2):315.
[14] Fauteux D. J Electrochem Soc 1987;134(11):2761.
[15] Fauteux D, McCabe P. Polymers for Advanced Technologies 1995;6:83.
[16] Gorecki W, Jeannin M, Belorizky E, Roux C, Armand M. J Phys: Condens Matter 1995;7:6823.
[17] Kim JY, Bae YC. accepted in Polymer, 1997.
[18] Bae YC, Shim JJ, Soane DS, Prausnitz JM. J Appl Polym Sci 1993; 47:1193.
[19] Qian C, Munby SJ, Eichnger BE. Macromolecules 1991;24:1655.
[20] Guggenheim EA. Phil Mag 1935;19(7):588.
[21] Guggenheim EA, Turgeon TJ. Trans Faraday Soc 1955;51:747.
[22] Flory PJ. In: Principles of polymer chemistry. Ithaca, NY: Cornell University Press, 1953.
[23] Qian C, Munby SJ, Eichnger BE. J Polym Sci Part B 1991;29:635.
[24] Barton AF. In: Handbook of solubility parameters and other cohesion parameters. Boca Raton, FL: CRC Press, 1983.